Cerebral Cortex, December 2015;25: 4898–4907

doi: 10.1093/cercor/bhv212
Advance Access Publication Date: 25 September 2015
Original Article

ORIGINAL ARTICLE

Prestimulus Network Integration of Auditory Cortex Predisposes Near-Threshold Perception Independently of Local Excitability

Sabine Leske[1], Philipp Ruhnau[2], Julia Frey[2], Chrysa Lithari[2], Nadia Müller[3], Thomas Hartmann[2] and Nathan Weisz[2]

[1]Department of Psychology, University of Konstanz, 78457 Konstanz, Germany, [2]Center for Mind/Brain Sciences (CIMeC), University of Trento, 38123 Mattarello (TN), Italy and [3]Department of Neurology, Epilepsy Center, University Hospital Erlangen, 91054 Erlangen, Germany

Address correspondence to Sabine Leske, Department of Psychology, University of Konstanz, Pf. 905, 78457 Konstanz, Germany.
Email: sabine.jatzev@gmail.com

Abstract

An ever-increasing number of studies are pointing to the importance of network properties of the brain for understanding behavior such as conscious perception. However, with regards to the influence of prestimulus brain states on perception, this network perspective has rarely been taken. Our recent framework predicts that brain regions crucial for a conscious percept are coupled prior to stimulus arrival, forming pre-established pathways of information flow and influencing perceptual awareness. Using magnetoencephalography (MEG) and graph theoretical measures, we investigated auditory conscious perception in a near-threshold (NT) task and found strong support for this framework. Relevant auditory regions showed an increased prestimulus interhemispheric connectivity. The left auditory cortex was characterized by a hub-like behavior and an enhanced integration into the brain functional network prior to perceptual awareness. Right auditory regions were decoupled from non-auditory regions, presumably forming an integrated information processing unit with the left auditory cortex. In addition, we show for the first time for the auditory modality that local excitability, measured by decreased alpha power in the auditory cortex, increases prior to conscious percepts. Importantly, we were able to show that connectivity states seem to be largely independent from local excitability states in the context of a NT paradigm.

Key words: auditory consciousness, functional connectivity, graph theory, MEG, ongoing oscillations

Introduction

The importance of investigating large-scale interactions between neuronal ensembles, to understand the neural mechanisms supporting cognition, is becoming generally recognized. With regards to the so-called neural correlates of consciousness (NCC; Crick and Koch 1998), an increasingly important view asserts that conscious perception of sensory stimuli requires recurrent communication between a distributed set of brain regions, involving—in the case of full (i.e., reportable) awareness—fronto-parietal areas (Lamme 2006; Dehaene and Changeux 2011).

However, when it comes to the prerequisites of conscious perception (Aru et al. 2012), research so far has stressed mainly prestimulus local excitability in early sensory regions. In particular, experiments using NT stimuli showed reduced prestimulus

alpha power—an index of the cortical excitation level—prior to a conscious percept in relevant sensory regions involved in processing the upcoming stimulus (Ergenoglu et al. 2004; Hanslmayr et al. 2007; Romei et al. 2008; Van Dijk et al. 2008; Lange et al. 2013; Ruhnau et al. 2014). Furthermore, Sadaghiani et al. (2009) reported enhanced prestimulus BOLD (blood oxygen-level dependent) contrast prior to hits in an auditory NT task, which aligns with the view that alpha-band power (~8–14 Hz) states are inversely related to excitability states of respective neural ensembles (see Klimesch et al. 2007; Jensen and Mazaheri 2010 for reviews).

On the other hand, several studies demonstrated that early local excitability changes in sensory regions in the "poststimulus" period do not differentiate between conscious and unconscious perception (Dehaene et al. 2006; Lamme 2006; Dehaene and Changeux 2011). However, this should be the case (e.g., because neurons are closer to firing threshold prior to hits) if prestimulus excitability of sensory cortical areas is the main determining factor for conscious perception in a NT paradigm (for details on the rationale, see Ruhnau et al. 2014). Thus, it is likely that additional mechanisms other than prestimulus excitability contribute to upcoming conscious perception.

Accordingly, for the poststimulus interval, there is a growing consensus that early neural activity related to the stimulus representation in sensory regions (i.e., not driven by recurrent activation from higher order areas) alone does not determine whether a stimulus will become reportable, but only when it is embedded in a network (Lamme 2006). This view finds support in studies showing enhanced functional connectivity in the poststimulus interval for consciously perceived stimuli (Melloni et al. 2007; Palva and Palva 2012).

The aim of the present MEG study was to scrutinize this issue in further detail and investigate the contribution of prestimulus local excitability and connectivity dynamics to conscious perception of upcoming weak auditory stimuli. In a previous somatosensory NT task, we demonstrated not only reduced prestimulus somatosensory alpha power prior to hits, but also an increased network-level integration of this region, as operationalized via diverse graph theoretical measures (Weisz et al. 2014). This finding formed the basis of our framework ("Windows to Consciousness," Win2Con; see also Ruhnau et al. 2014), which states that for a NT stimulus to become consciously perceived, sensory essential nodes (Zeki and Bartels 1999) require pre-established pathways along which weak sensory information can impact downstream regions. Here, we used an auditory NT task and report for the first time prestimulus alpha power and network effects in the auditory modality with patterns akin to previous NT reports in other modalities (Van Dijk et al. 2008; Sauseng et al. 2009). In particular, we attempt to go beyond our previous work and show that the network, as well as poststimulus effects, remains robust following a stratification of hit and miss trials for alpha power. This implies that connectivity states are largely independent of local excitability in auditory areas with respect to their influence on the perceptual fate of an upcoming NT acoustic stimulus.

Materials and Methods

Participants

Nineteen healthy volunteers participated in the current study. Of those, 2 participants were excluded from the analysis due to excessive artifacts in the MEG data and 3 participants were excluded because their individual threshold could not be estimated reliably. The remaining 14 participants (mean age: 29.71, SD: 5.7 years; 6 female; 13 right handed) reported normal hearing and vision. Participants gave written informed consent and received 40€ at the end of the experiment. Ethical approval was obtained from the University of Trento Ethics Committee.

Stimulus Material and Procedure

Auditory stimuli were presented binaurally over tubal insert earphones (VIASYS, CareFusion Corporation, 3750 Torry View Court, San Diego, CA 92130, USA, http://www.carefusion.de/medical-products/carefusion-brands/viasys/, last accessed on 9 September 2015). Short burst of white noise with a length of 100 ms was generated with Matlab and multiplied with a Hanning window to obtain a soft on- and offset. Participants had to detect short white noise bursts presented near hearing threshold. A staircase procedure (Von Békésy 1960) was conducted at the beginning of the experimental session to determine the loudness level, ensuring approximately 50% detection rate. In the following session, participants performed the auditory detection task and were instructed to keep their eyes open, fixate on a white cross, and to press the button with their right index finger as soon as they heard a noise.

The central white fixation cross on gray background remained on screen throughout the experimental block, preventing the participant becoming aware of a noticeable trial structure. Hence, participants had no information about stimulus timing. The inter-trial interval (ITI) varied between 3000 and 6000 ms and was drawn from a random gamma distribution, ensuring that the stimulus onset was difficult to predict by the participant (Fig. 1). There were 3–5 blocks of 100 trials each (10% catch trials presented above hearing threshold, +10 dB), resulting in 300–500 trials in total. The whole experiment lasted for ~2 h.

Trials were classified into hits (detected) and misses (undetected stimulus). Trials with reaction times <1000 ms in regard to stimulus onset were classified as hits, and trials with no responses within this time window were classified as misses. Responses outside the given time window were classified as False Alarms. The auditory NT experiment was programmed in Matlab using the open source Psychophysics Toolbox (Brainard 1997).

Data Acquisition

MEG data were recorded at a sampling rate of 1 kHz with a 306-channel (204 first order planar gradiometer, 102 magnetometers) whole-head VectorView MEG system (Elekta-Neuromag Ltd., Helsinki, Finland). Participants sat in a magnetically shielded room (AK3B, Vakuumschmelze, Hanau, Germany). The MEG signal was band-pass filtered in the frequency range of 0.01–330 Hz by accordingly adjusted hardware filters. Prior to the experiment head position indicator (HPI), coils were attached to the scalp of participants, and the head shape and landmarks like nasion, inion, Cz, left and right ear canal of participants were digitized using a Fastrak 3D digitizer (Polhemus, Colchester, VT, USA, http://www.

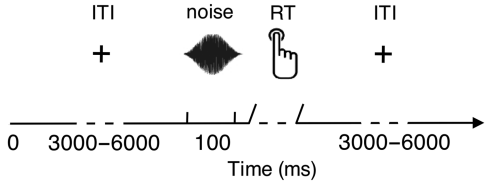

Figure 1. Timeline of a sample trial of the experimental paradigm.

polhemus.com, last accessed on 9 September 2015). During the experiment, participants were comfortably seated under the MEG helmet and instructed to keep the head still and avoid movements.

MEG Data Analysis

Data were filtered using a 1 Hz high-pass Butterworth filter (zero phase, IIR, filter order 6), visually inspected to exclude trials contaminated by ocular, muscle or other MEG artifacts and down-sampled to 512 Hz. Sensors that contained channel jumps or artifacts were excluded from further analysis. To ensure a comparable signal-to-noise ratio between conditions (hits and misses), the trial number was equalized by randomly excluding trials. This resulted in a mean of 90.57 trials per condition (range: 75–155) and a mean of 181.14 trials in total.

To enable a time–frequency representation in source space of all measures, single trial time series were projected into source space via a spatial filter obtained by linearly constrained minimum variance (lcmv) beamforming analysis (Van Veen et al. 1997), thereby obtaining virtual sensor time series. The respective spatial filter was based on the covariance matrix of the 4–30 Hz band passed signal (zero phase Butterworth filter, IIR, filter order 6), for a time window ranging from −800 to 600 ms. The only exception is the preprocessing of the data for the spatial filter used to obtain source event-related fields. Here no high-pass filter was applied, and the data were 30 Hz low-pass filtered before calculating the covariance matrix. Source reconstruction included magnetometers as well as gradiometers. For this purpose, the balancing matrix was divided by a factor of 0.017 for the gradiometers prior to the calculation of the leadfield matrix. Template Montreal Neurological Institute (MNI) brain aligned grids in individual headspace were created as described in the following. A 3D grid covering the entire brain volume (resolution of 1.5 cm) was created based on a standard MNI template MRI. Since there were no individual MRIs available, personalized *MRIs* were created by warping the standard MRI to optimally match the individual head shape. The MNI space equidistantly placed grid was then morphed to individual headspace. Leadfields were calculated for each participant based on a single-shell model (Nolte 2003) of the brain. Subsequent data analysis was based on the obtained source-space (virtual sensor) time series.

Analysis of MEG data was accomplished using the Matlab-based open source Fieldtrip toolbox (Oostenveld et al. 2011), the Brain Connectivity Toolbox (Rubinov and Sporns 2010) and custom-made Matlab functions.

Evoked Response Analysis

Evoked responses were obtained for the entire source space by averaging single trial data for the pre- and poststimulus time range (−500 to 500 ms). A baseline normalization was applied for the absolute values of the event-related fields, including the time range of −300 to 0 ms as baseline window.

Frequency Power Analysis

To transform data into frequency domain (4–30 Hz, in steps of 2 Hz), a Fast Fourier Transformation (FFT) was applied to virtual sensor single trial time series by using frequency adaptive Hanning-tapered sliding time windows (time window for taper: $\Delta t = 5$ cycles/frequency, sliding in steps of 50 ms).

Graph Theoretical Analysis

Graph theoretical measures were calculated on graphs derived from functional connectivity analysis in source space. All-to-all connectivity analysis was based on the single trial source-space time series (see above: MEG Data Analysis) for the prestimulus period (−600 to −100 ms). Respective virtual sensor data were Fourier transformed using a multitaper FFT (discrete prolate spheroidal sequences—DPSS, 3 tapers $\Delta f = 4$, Bell et al. 1993) with a frequency adaptive time window ($\Delta t = 5$ cycles/frequency), sliding in steps of 100 ms. The frequency range included 4–30 Hz in steps of 2 Hz. This yielded time–frequency resolved complex Fourier values in source space as a basis for the calculation of coherence. The imaginary part of coherence (IC) was derived for each dimension (source × source × frequency × time) and used as a connectivity metric (Nolte et al. 2004). IC is a conservative measure not prone to spurious interactions between cortical areas, which are caused by volume conduction.

To obtain a binary adjacency matrix (zeros indicating absence, ones indicating the presence of a functional connection) for graph theoretical analysis, the all-to-all connectivity matrix needs to be thresholded. There is no objective way to decide the threshold value in graph theoretical approaches (Van Wijk et al. 2010). The threshold was chosen individually for each frequency and participant by selecting the highest possible IC value, ensuring no disconnected nodes in the graph, and the respective minimum of both conditions. The resulting binary adjacency matrices were used for graph theoretical analysis.

To quantify local connectivity, the brain network measures "node degree" and "betweenness centrality" were selected. The degree of a node is the number of edges connected to the node and therefore identifies brain regions that are interacting with many other regions in the brain network (Rubinov and Sporns 2010). Betweenness centrality is defined as the fraction of all shortest paths in the network passing through that node. The description "shortest paths" does not relate to physical distance, but the least number of nodes that have to be passed, to pass information from one node to the other. This applies especially for areas that are bridging distant regions in the brain, likewise the according cortical area conveys a vast amount of the information flow (Rubinov and Sporns 2010). Both measures assess the importance of nodes within a network, possibly identifying hubs, that is, brain regions that facilitate functional integration and interact with many other regions (Rubinov and Sporns 2010).

As a region of interest (ROI), the primary auditory cortex (AI) was chosen and the respective MNI coordinates of Brodmann Area 41 and 42 (BA 41, 42) were identified with an anatomical brain atlas (AFNI TTatlas, http://afni.nimh.nih.gov/afni/doc/misc/afni_ttatlas/, last accessed on 9 September 2015). Grid points (MNI space) closest to BA 41 and 42 coordinates were identified via method of least squares, resulting in 10–12 grid points per ROI (see Supplementary Fig. 1). The local graph theoretical measures node degree and betweenness centrality were derived for this AI ROI for each hemisphere. For visualization purposes, the time–frequency range showing significant differences in groups statistics for node degree and betweenness was chosen to map the cortical distribution of the condition contrast (normalized difference) of the respective graph theoretical measure across the whole brain (thresholded at $P < 0.025$, uncorrected).

To visualize the spatial connectivity patterns underlying these graph theoretical effects, grid points were chosen as seeding regions to map functional connectivity (imaginary coherence) from this region to the rest of the brain. The grid point (virtual sensor) showing the maximum value for the group-level statistics for node degree was identified for the right and for the left auditory cortex. For the respective virtual sensor, the time–frequency point with the maximum statistical value for node degree was selected to map the condition contrast for imaginary coherence across the whole brain (nonparametric

dependent samples *t*-test). Respective statistical values were thresholded at $P < 0.05$ (2 sided, uncorrected) and interpolated onto the standard MNI brain to reveal brain regions that are coupled or decoupled from the seeding grid point.

Alpha Power Stratification

Single trials for the conditions hits and misses were equated with respect to alpha-band power for each participant separately. For each trial, the mean power in the classical alpha band, as it is commonly defined in literature (8–12 Hz), and the prestimulus interval (−600 to −100 ms) were calculated (for frequency analysis see above). Our intention was to compare the relative contribution of prestimulus excitability levels and connectivity to perception. The choice of the frequency band ensured that the stratification included the alpha-band range (8–12 Hz) that is referred to by other studies as reflecting functional inhibition (or excitability levels) influencing conscious perception (see Klimesch et al. 2007; Jensen and Mazaheri 2010 for reviews). The grid point showing the maximal statistical power effect within the AI ROI was selected for stratification with respect to alpha power as described in the following. The distributions of both conditions were equated regarding the mean, variance and all higher order statistics, by including only those bins of the distribution that overlap. The bin width was defined to include 15 trials, which seemed adequate regarding the total number of trials ranging from 100– to 200 trials per participant. The small within-bin bias that occurs due to the distributions being shifted was not removed. As a sanity check, a group statistical analysis was repeated on stratified power data to ensure that the power effect (hit vs. miss) disappeared. The same trials (stratified data) were selected to recalculate the graph theoretical measure node degree for the right auditory cortex to test whether network contrast effects persist after alpha power stratification. This also nicely controls for confounding effects of different signal-to-noise ratios due to condition differences in source power.

Statistical Analysis

The prestimulus period (−600 to 0 ms) was considered in comparing MEG patterns discriminating between hits and misses before NT stimulus arrival. The statistical contrast for source power included a frequency range of 4–30 Hz (steps of 2 Hz) and the entire grid space. For graph theoretical measures, the alpha-band range (8–16 Hz, steps of 2 Hz), the prestimulus period (−600 to −100 ms, steps of 100 ms) including the strongest modulation of the significant source power effect, and the AI ROIs were selected as input range for the statistical contrast. Since primary auditory cortices are spatially separated (and cannot form a coherent cluster), statistical tests were conducted for left and for right AI separately.

If not stated otherwise, the conditions hits and misses were contrasted via group statistical analysis using nonparametric cluster-based permutation tests with a Monte Carlo randomization (Maris and Oostenveld 2007) across time, frequency and grid points, controlling for multiple comparisons. As a metric, the normalized difference between conditions (A−B)/(A+B) was computed (Spaak et al. 2014), following a decadic logarithmic transformation of the data (the only exception is the betweenness centrality measure). To obtain clusters, the 95th percentile of the permutation distribution of the conditions (1000 permutations) for this metric was used to threshold the observed values for each dimension individually (virtual sensor–time–frequency). The final permutation distribution was based on the cluster candidates of each permutation, with the highest sum of normalized difference. The sum of descriptives (here the normalized difference) for the observed cluster candidates was compared with this cluster permutation distribution. Clusters fulfilling the $P < 0.05$ criterion (2-sided test) were considered statistically significant.

Statistical testing of the evoked responses effect was based on the poststimulus time range (0–500 ms) and restricted to bilateral AI ROI, using dependent samples *t*-tests and nonparametric cluster-based permutations with a Monte Carlo randomization (Maris and Oostenveld 2007), controlling for multiple comparisons.

Statistical re-analysis of power, evoked response, and graph theoretical results after alpha power stratification was conducted by selecting the data point with the maximum statistical value in time–frequency–grid space for the original data (before stratification) and calculating a dependent sample *t*-test.

Source space statistical values (thresholded at $P < 0.05$, 2-sided; uncorrected) were interpolated onto an MNI brain for visualization purposes. Source space data were visualized using surface renderings.

Results

Behavioral Results

Across all participants, the average percentage of hits (detected stimuli) was 41% (±17%). This rough balance between hits and misses is comparable to other auditory threshold studies (Sadaghiani et al. 2009). The false alarm rate was low overall, with a mean of 8% false alarms (average percentage per total events) per session and a standard deviation of 5%.

Poststimulus Modulations: Evoked Responses

To compare poststimulus processing for hit and miss trials, evoked responses were calculated for the entire grid space. The statistical condition contrast (hits minus misses) of the poststimulus time range (0–500 ms) included grid points of AI ROIs.

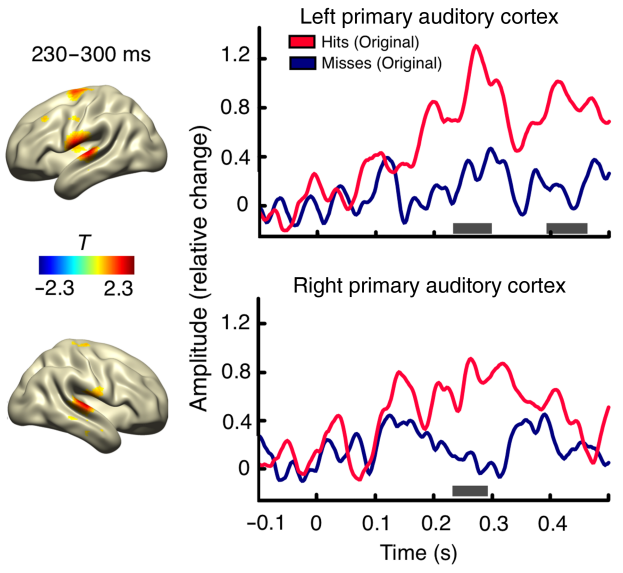

Figure 2. Source level evoked responses for hits and misses. The spatial distribution of *T*-values for the statistical contrast (hits minus misses) is shown (left side) for the significant time period ranging from 230 to 300 ms (masked at $P < 0.05$). Time series are shown for evoked responses of hits (red) and misses (blue) for ROIs (left and right AI). Significant time periods are indicated with gray lines.

Nonparametric cluster-based permutation tests revealed significant differences for the evoked responses in the regions of interest for rather late peaks (see Fig. 2): right ($P = 0.02$; 230–300 ms) and left auditory cortex (first cluster: $P = 0.008$, 230–300 ms; second cluster: $P = 0.022$, 390–470 ms).

For the visualization of the spatial distribution of the statistical contrast of the event-related fields, statistical T-values of the ERF effects were mapped across the whole cortex for the time range showing significant differences between hits and misses, masked at $P < 0.05$ (uncorrected; Fig. 2). This confirmed that the strongest condition contrast is indeed revealed for AI of both hemispheres.

Prestimulus Power Modulations

To relate prestimulus fluctuations in spectral power to auditory detection performance, the prestimulus (–600 to 0 ms) theta- to beta-band (4–30 Hz) spectral power estimates (Fig. 3) were entered into a nonparametric cluster-based permutation test (hits vs. misses). This resulted in a negative cluster ($P = 0.008$, corrected) with local peaks in both primary and middle occipital cortices (VI, Ba 17, BA 18, 19) and the right auditory cortex [AI, BA 41 and 42, Superior Temporal Gyrus (STG), BA 22]. For the right auditory cortex, a significant prestimulus (–600 to 0 ms) power reduction in the alpha- and beta-band range (6–20 Hz) was revealed (Fig. 3), which showed the strongest modulation in the alpha band (8–14 Hz). The same cluster-based statistical analysis was conducted on grid points of the ROI (right AI) to ensure that this auditory region shows a genuine alpha power effect. This confirmed significant prestimulus alpha power reductions for hits (data not shown). In sum, auditory perceptual awareness was mainly characterized by significant prestimulus alpha-band power reductions in the right auditory cortex and visual cortices of both hemispheres.

Prestimulus Brain Network Fluctuations

Graph theoretical analysis served as a method to describe prestimulus brain network states, potentially influencing upcoming auditory perception of the NT stimulus. Bilateral AI was selected as ROIs to elaborate perception-relevant network dynamics. The corresponding grid points were identified to extract local graph theoretical estimates for node degree and betweenness centrality for the selected prestimulus time–frequency interval (–600 to –100 ms; 4–30 Hz). The respective cluster-based permutation statistics included the prestimulus alpha-band range (8–16 Hz), which already showed significant prestimulus power fluctuations (see above).

The Win2Con framework (Weisz et al. 2014; outlined in the introduction) predicts an enhanced integration of essential nodes (in this study: auditory cortices) in the brain functional network, predisposing communication with other brain areas. This was confirmed by relatively increased node degree before hits for the left auditory cortex ($P = 0.019$, corrected), encompassing the upper alpha band (10–16 Hz) and a time window ranging from –600 to –200 ms (Fig. 4A). To give a descriptive characterization of the underlying connectivity pattern, the grid point with the maximum statistical value (node degree contrast) in left AI was used as a seed region, to map the spatial distribution of imaginary coherence at 12 Hz and –400 ms (statistical maximum in time–frequency space) across the cortex. These results reveal that the node degree effect for left AI was mainly driven by an enhanced communication to the right middle temporal gyrus (BA 21), a region involved in auditory processing (Fig. 4B). Furthermore, the left auditory cortex showed enhanced prestimulus coupling to a fronto-parietal network, encompassing right prefrontal (BA 46, 10), left superior frontal gyrus (BA 8, 9), left superior parietal (BA 7), and left inferior parietal lobule (BA 40).

In addition to the enhanced connectivity between auditory regions of both hemispheres, prestimulus network dynamics were characterized by significantly increased betweenness centrality for left AI ($P = 0.011$), encompassing a time–frequency range (10–14 Hz, –600 to –300 ms; Fig. 5) very similar to the node degree effect (Fig. 4A). This indicates that many shortest paths of the network pass through left AI, confirming its role as a hub in the brain network with respect to auditory stimulus detection.

Surprisingly, the right auditory cortex showed the inverse effect: a significant prestimulus decrease in node degree prior to hits ($P = 0.004$) relative to misses for a slightly different frequency range of 8–12 Hz, but for a similar time range (–600 to –400 ms; Fig. 4A). The underlying connectivity pattern of this effect revealed that this is driven by a decoupling of the right auditory cortex from the left and right prefrontal and inferior frontal gyrus (BA 9, 45), left precentral gyrus (BA 6), inferior parietal lobule (BA 40), left middle and inferior temporal gyrus (BA 21, 20), and, interestingly, occipital regions (Lingual Gyrus, Culmen, BA 18, 19) (Fig. 4B). Note that the experimental task context implies that the visual input carries no information regarding the auditory stimulus timing and is therefore irrelevant for the task goal.

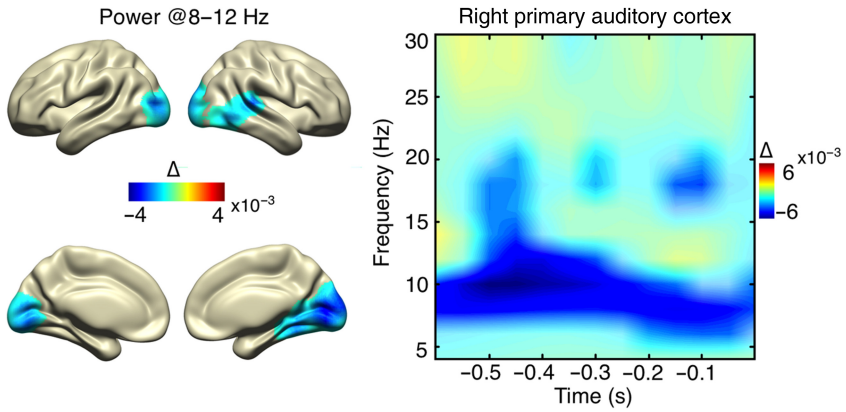

Figure 3. Prestimulus source power modulations. The spatial distribution of relative change in power encompassing the significant time–frequency range (8–12 Hz, –600 to 0 ms) is shown on the left and the respective time–frequency distribution for the right AI on the right (significance marked with opaque colors), revealing a relative prestimulus decrease in alpha power for detected stimuli.

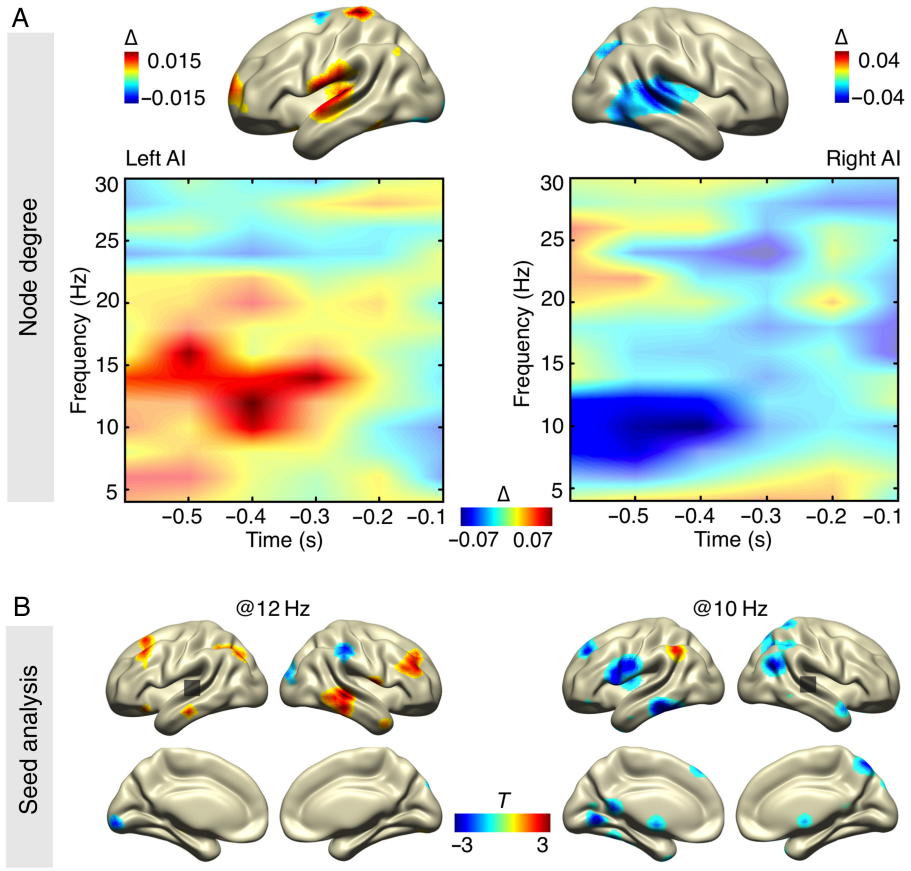

Figure 4. Prestimulus network modulations. (*A*) The time–frequency representation of node degree (normalized change values) reveals a relative increase for detected stimuli (significance marked with opaque colors) for the left auditory cortex and a decrease for the right auditory cortex (in both cases spatial statistical maximum) in the alpha-band range (lower panel). Spatial mapping of significant time–frequency ranges (masked at $P < 0.05$, uncorrected) shows that sources for these effects are mainly situated in auditory cortices (upper panel). (*B*) Underlying connectivity patterns (masked at $P < 0.05$, uncorrected) for node degree effects are shown for seeds in left and right auditory cortex (statistical maximum in time–frequency–source space). The relative increase in node degree is mainly driven by an enhanced bilateral coupling between auditory processing regions of both hemispheres.

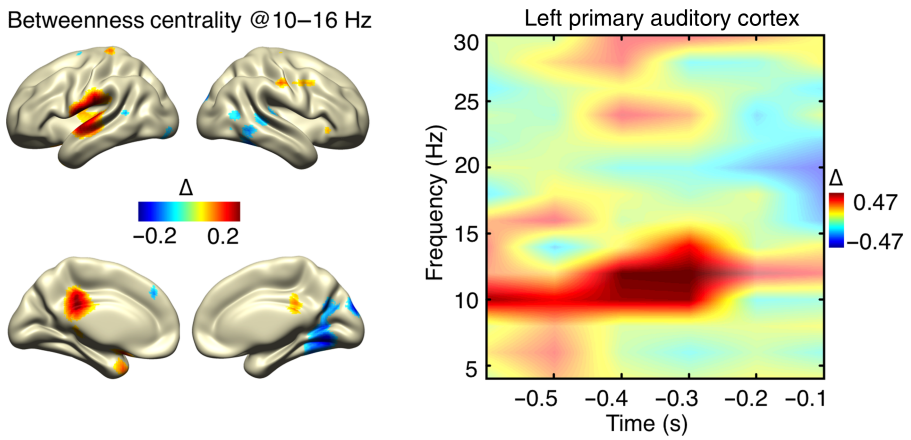

Figure 5. Prestimulus betweenness centrality effects. The time–frequency representation of betweenness centrality (normalized change values) for the left auditory cortex (spatial statistical maximum) shows a relative increase for detected stimuli (significant values are marked with opaque colors). Spatial mapping of the significant time–frequency range reveals the main source in the left auditory cortex and an additional source in the posterior cingulated cortex.

For a spatial distribution of these graph theoretical contrasts (hits vs. misses, normalized change), see Figures 4A and 5. Node degree and betweenness centrality show a strong spatial overlap regarding the left auditory cortex (Figs 4A and 5). The spatial mapping also confirmed that network modulation effects in the alpha frequency range (8–16 Hz) were indeed primarily confined to auditory regions (STG, BA 41 and 42). An exception is the betweenness centrality effect (Fig. 5). Here an effect was

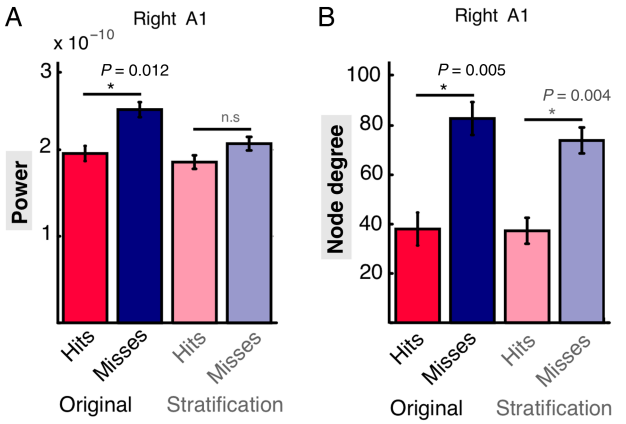

Figure 6. Stratification of alpha power. (*A*) Source power values for the statistical maximum in time–frequency–grid space, before (Original) and after alpha power stratification. The significant reduction in prestimulus alpha power vanishes after stratifying for alpha power. (*B*) Node degree values for the statistical maximum in time–frequency–grid space, before and after stratification of alpha power for the right auditory cortex. Significant differences between hits and misses persist after alpha power stratification.

also visible for the posterior cingulate cortex (BA 23, 31). It has to be noted that, although source-level power analysis revealed strong significant prestimulus effects for the primary visual cortex (BA 17, see Fig. 2*B*), interestingly, corresponding effects are absent or negligible for node degree.

In summary, these results reveal that a complex interplay of prestimulus enhanced local excitability—in this case in the right auditory cortex—and an enhanced integration of a sensory region into the neural network—here the left auditory cortex—favors perception of an upcoming weak perceptual stimulus. Importantly, this network configuration includes an increased connectivity between auditory processing regions of both hemispheres prior to conscious perception, while remarkably the right auditory cortex is characterized by a broad decoupling from other brain regions.

Stratification of Alpha Power

The main findings so far already show that there is no simple relationship between prestimulus local excitability of sensory areas (here, right AI), indexed via reduced alpha power, and the connectivity of these regions. The right auditory cortex shows a decrease in power (possibly reflecting increased excitability), but also a decrease in node degree, hence a strong relative decoupling from a wide set of distributed areas prior to hits. To test the extent that reduced connectivity effects were independent from local excitability effects, trials of both conditions were equalized with respect to alpha power (Fig. 6 and see Supplementary Fig. 2). This analysis also controls for the theoretical possible scenario of connectivity effects being introduced by different signal-to-noise levels at the same frequency due to source power differences between conditions. Overall, roughly 17% of trials had to be removed to yield similar alpha power levels; the resulting distributions in 2 participants can be seen in Supplementary Figure 2.

Statistical re-analysis of the stratified power and graph theoretical results was conducted for the statistical maximum in time–frequency–grid space of the original results (before stratification) using dependent samples *t*-tests. As expected, the significant statistical difference in alpha power between both conditions disappeared (Fig. 6*A*) for the right auditory cortex ($P = 0.2$). Nevertheless, network effects for node degree for the right auditory cortex ($P = 0.004$) remained significant after stratification (Fig. 6*B*). Thus, the prestimulus connectivity architecture is likely independent of the power modulations in influencing awareness of the upcoming auditory NT stimulus. Interestingly, significant differences in evoked responses did remain after alpha power stratification and showed a morphology very similar to the original data. For the right auditory cortex, significant differences were again revealed between 250 and 340 ms ($P = 0.014$) and for the left auditory cortex between 230 and 290 ms (first cluster: $P = 0.016$) and 400 and 470 ms (second cluster $P = 0.048$, data not shown).

Discussion

The present work is based on our recent framework (Ruhnau et al. 2014; Weisz et al. 2014), which aims to identify and characterize prestimulus functional networks, shaping predefined pathways and guiding upcoming information flow necessary for perceptual consciousness. Within this framework, we predicted that auditory awareness is preceded not only by regional excitability changes, but rather by an enhanced integration of relevant sensory areas ("essential nodes"; Zeki and Bartels 1999) into the brain functional network, forming pre-established pathways of neuronal communication (windows to conscious perception) and reducing the degree of freedom of information flow in the network (Weisz et al. 2014).

We used an auditory NT task, without a noticeable trial structure, and therefore, NT stimuli were temporally unpredictable for the participant (Sadaghiani et al. 2009). Overall, our results provide strong evidence for the Win2Con framework. They reveal prestimulus excitability and functional network configurations that predict the perceptual fate of an auditory NT stimulus. These network dynamics revealed an interesting and complex implementation of the proposed pre-established information routes enabling perceptual awareness. Task-relevant sensory processing regions, in this case the left auditory cortex (BA 41, 42, Superior Temporal Gyrus), showed an enhanced integration into the functional network for detected auditory stimuli. Taking a central position in the network configuration, this region showed enhanced prestimulus node degree and betweenness centrality, indicative for hub structure in a network (Rubinov and Sporns 2010).

The spatial overlap of the node degree and betweenness centrality effect implies that the left AI not only exhibits an increased number of connections, but also that these additional connections constitute the shortest paths in the brain network. This indicates that this region is crucially important in mediating information flow prior to a conscious auditory percept, thereby contributing to a brain functional network biased toward auditory NT stimulus detection.

At the same time, the right auditory cortex showed as expected increased prestimulus excitability, but significantly reduced prestimulus network integration, visible via decreased node degree prior to hits, which was not predicted by the Win2Con framework. In the following, these lateral asymmetries in network configurations and possible implications for the framework will be discussed.

Network States and Underlying Connectivity Patterns

Seeded connectivity revealed that enhanced node degree and betweenness centrality of the left auditory cortex were based on an increased coupling between auditory processing regions of both

hemispheres (left Superior Temporal Gyrus and right Middle Temporal Gyrus); a neuronal communication pattern that likely enhances efficiency of upcoming auditory information processing. Interestingly, the functional relevance of fast auditory inter-hemispheric interaction is also evidenced by the structural inter-hemispheric auditory pathways, which are among the densest and have the largest fiber diameters of the corpus callosum, consequently possessing fast conduction velocities (Aboitiz et al. 1992; Steinmann et al. 2014).

The strongly enhanced connectivity of the left versus the right auditory cortex supports the notion that the left AI seems to take control of processing resources of right auditory brain regions, forming an enlarged and integrated information processing unit. Since the experimental task in our study emphasizes stimulus timing rather than spectral stimulus properties, this nicely fits with studies investigating hemispheric asymmetries. Left auditory cortical areas have been proposed to have a higher degree of temporal resolution with respect to stimulus processing (Belin et al. 1998; Zatorre 2001) in contrast to right auditory areas, which seem to show greater spectral sensitivity. Structurally, the left AI seems to possess a greater number of larger cells with more heavily myelinated axons, greater interconnectivity and a greater volume of white matter underlying the Heschl's gyrus compared with the right auditory cortex (Seldon 1981a, b, 1982; Hutsler and Gazzaniga 1996; Penhune et al. 1996; Zatorre et al. 2002), which would facilitate faster transmission of information. Following this line of thought, the decoupling of the right auditory cortex could be interpreted as redirecting the information flow from the right to the left auditory cortex, which is specialized for the task at hand and connects to the rest of the brain network.

The current results reveal a network configuration that is in line with the predictions made by the Win2Con framework, which states an increased coupling from sensory to perception-relevant fronto-parietal areas. The exact implementation of these connectivity patterns and therefore the according graph theoretical effects can be diverse and therefore cannot be directly deduced from the framework.

Therefore, the reason for the unexpected lateral asymmetry of the excitability and network effects in both auditory cortices remains open. The reduced network integration and connection sparseness of the right auditory cortex might provide protection against interference from other brain areas. The relevance of precluding communication to neuronal groups representing irrelevant stimulus information has already been pointed out by several authors (Fries 2005; Singer 2011; Palva and Palva 2012) and has been related to oscillatory properties, for example, implemented via an absence of phase consistency between oscillations of different brain areas (Fries 2005). In the current study, the reduced network integration of the right auditory cortex might also constitute an important preclusion of irrelevant information from other areas.

Simultaneously, the enhanced coupling of right auditory regions to a task-relevant central hub of the network (left auditory cortex) ensures the propagation of the stimulus presentation to higher order processing regions of the brain.

This interpretation would nicely fit with the identified increased coupling from the left auditory cortex to frontal and parietal areas (Superior Frontal Gyrus and Superior Parietal Gyrus). A prestimulus network configuration was revealed that has already been proven to be relevant for conscious access with respect to poststimulus information processing. Numerous studies have shown that stimulus information has to be shared among widespread areas beyond sensory regions, involving a fronto-parietal network (Lamme 2006; see also Dehaene and Changeux 2011, for the neuronal global workspace model). Our results provide strong evidence that crucial pathways are already defined before stimulus arrival to efficiently guide information flow, as predicted by the Win2Con framework (Ruhnau et al. 2014; Weisz et al. 2014).

Network States and Local Excitability

In line with previous studies investigating prestimulus activity influencing perceptual awareness, this study revealed reduced prestimulus alpha power, but only for the right A1, possibly reflecting enhanced excitability (Ergenoglu et al. 2004; Hanslmayr et al. 2007; Romei et al. 2008; Van Dijk et al. 2008; Weisz et al. 2014).

Next to reduced alpha activity in the right auditory cortex, both primary visual cortices showed a decrease in alpha power prior to stimulus detection. This effect could also mirror enhanced excitability of the visual system, which was not expected from the task context. A possible reason for this could be the fact that under natural conditions auditory and visual stimuli often carry conforming information about the same object, and the combination of information from both modalities usually generates perceptual advantages (Bulkin and Groh 2006). Multimodal studies have convincingly shown an impact of auditory stimuli on early visual processing (Romei et al. 2012; Lange et al. 2014; Cecere et al. 2015) or the visual dominance over auditory perception in spatial localization (Knudsen and Brainard 1995; Recanzone 2003). Also the McGurk illusion is an example how a multimodal percept can be distorted by the early neuronal integration of inconsistent visual and auditory information (Keil et al. 2012). Interestingly, multimodal studies suggest that often unimodal brain regions participate crucially in multisensory perception (Bulkin and Groh 2006), which could be an indication for the current results. Since the present study did not investigate multimodal interaction, these interpretations remain speculative. Importantly, however, the visual system did not show corresponding effects in graph theoretical or connectivity analysis, as was found for the auditory system, which demonstrates nevertheless a modality-specific prestimulus network configuration favoring auditory conscious perception.

Surprisingly, a significant alpha power reduction could not be revealed for the left auditory cortex. The exact reason for the hemispheric asymmetry is unknown, but interestingly hemispheric asymmetries have already been revealed in the auditory domain with respect to attention. Studies investigating spatial auditory attention and audiovisual spatial attention reported a dominance of the right auditory cortex with respect to attention-related alpha power modulations (Müller and Weisz 2012; Frey et al. 2014). This was interpreted as mirroring the already reported right hemispheric involvement in directing attention to both hemispheres (Zatorre and Penhune 2001; Corbetta and Shulman 2002; Müller and Weisz 2012). This might also be a possible explanation for the current asymmetry of the auditory cortices in alpha power reduction and excitability.

But surprisingly (see, Popov et al. 2013), in the current study, the right auditory cortex showed—next to reduced alpha power—a relatively reduced connectivity to other brain regions before stimulus arrival (see also the discussion above), indicated by decreased node degree. Accordingly, reduced alpha power, or enhanced excitability, of sensory regions does not necessarily coincide with overall enhanced connectivity to other areas.

In particular, we investigated whether prestimulus local excitability and network integration are dependent on each other

in the context of our NT task. To test this, we stratified trials of both conditions with respect to prestimulus alpha power for the right auditory cortex, leaving no significant differences in prestimulus auditory alpha power between conditions. The right auditory cortex nevertheless showed decreased centrality in the network, marked by significantly reduced node degree, excluding trivial explanations of this network effect based on signal-to-noise considerations. Importantly, matching both conditions with respect to prestimulus alpha power left the poststimulus evoked response almost completely unaffected. This result provides strong evidence that the reduced prestimulus network integration of the right auditory cortex seems to be largely independent of the excitability level.

Limitations of the study include the fact that the investigation of the network effects was confined to a ROI, the auditory cortex. Even though all-to-all connectivity was calculated to estimate graph theoretical measures, the 3-dimensional depiction of network effects in time–frequency and grid–space yielded a high-dimensional feature space that had to be reduced. Therefore, we cannot exclude that other brain regions in different frequency bands play an additional role in predicting perceptual awareness of auditory NT stimuli. A further concern might be that poststimulus effects might influence the results of the prestimulus time period. This might be caused due to large integration windows needed for the estimation of Fourier coefficients at lower frequencies and due to a frequency smoothing of ±4 Hz that was applied here. Since most reported network effects included or started at 10 Hz (encompassing frequencies up to 16 Hz) and did not exceed −300 ms, the according longest integration window (833 ms at 6 Hz) would only extend up to approximately 100 ms into the poststimulus time window. In case of a contamination by the poststimulus period, a statistical maximum at this time range would be expected to bleed into the prestimulus time range, which is not indicated by the spectro-temporal pattern of the network effects. Therefore, we believe a bias of the prestimulus effect due to poststimulus activity is very unlikely.

Our results provide strong evidence for the Win2Con framework (Ruhnau et al. 2014; Weisz et al. 2014), demonstrating that pre-established information routes between auditory and fronto-parietal areas enable efficient processing of upcoming events and precede perceptual awareness. In addition, we were able to show that significant network modulations of the right auditory cortex, which were mainly characterized by a decoupling from non-auditory brain regions, persist after controlling for significant differences in prestimulus alpha power between conditions. This study provides evidence that local prestimulus excitability and network dynamics within one brain region are not necessarily dependent on each other.

Supplementary Material

Supplementary material can be found at: http://www.cercor.oxfordjournals.org/.

Funding

This work was supported by the European Research Council (WIN2CON; ERC StG 283404). Funding to pay the Open Access publication charges for this article was provided by the European Research Council (WIN2CON; ERC StG 283404).

Notes

Conflict of Interest: None declared.

References

Aboitiz F, Scheibel AB, Fisher RS, Zaidel E. 1992. Fiber composition of the human corpus callosum. Brain Res. 598:143–153.

Aru J, Bachmann T, Singer W, Melloni L. 2012. Distilling the neural correlates of consciousness. Neurosci Biobehav Rev. 36: 737–746.

Belin P, Zilbovicius M, Crozier S, Thivard L, Fontaine A, Samson Y. 1998. Lateralization of speech and auditory temporal processing. J Cogn Neurosci. 10:536–540.

Bell B, Percival DB, Walden AT. 1993. Calculating Thomson's spectral multitapers by inverse iteration. J Comput Graph Stat. 2:119–130.

Brainard DH. 1997. The psychophysics toolbox. Spat Vis. 10:433–436.

Bulkin DA, Groh JM. 2006. Seeing sounds: visual and auditory interactions in the brain. Curr Opin Neurobiol. 16:415–419.

Cecere R, Rees G, Romei V. 2015. Individual differences in alpha frequency drive crossmodal illusory perception. Curr Biol. 25:231–235.

Corbetta M, Shulman GL. 2002. Control of goal-directed and stimulus-driven attention in the brain. Nat Rev Neurosci. 3:201–215.

Crick F, Koch C. 1998. Consciousness and neuroscience. Cereb Cortex. 8:97–107.

Dehaene S, Changeux J-P. 2011. Experimental and theoretical approaches to conscious processing. Neuron. 70:200–227.

Dehaene S, Changeux J-P, Naccache L, Sackur J, Sergent C. 2006. Conscious, preconscious, and subliminal processing: a testable taxonomy. Trends Cogn Sci. 10:204–211.

Ergenoglu T, Demiralp T, Bayraktaroglu Z, Ergen M, Beydagi H, Uresin Y. 2004. Alpha rhythm of the EEG modulates visual detection performance in humans. Brain Res Cogn Brain Res. 20:376–383.

Frey JN, Mainy N, Lachaux J-P, Müller N, Bertrand O, Weisz N. 2014. Selective modulation of auditory cortical alpha activity in an audiovisual spatial attention task. J Neurosci. 34: 6634–6639.

Fries P. 2005. A mechanism for cognitive dynamics: neuronal communication through neuronal coherence. Trends Cogn Sci. 9:474–480.

Hanslmayr S, Aslan A, Staudigl T, Klimesch W, Herrmann CS, Bäuml K-H. 2007. Prestimulus oscillations predict visual perception performance between and within subjects. Neuroimage. 37:1465–1473.

Hutsler JJ, Gazzaniga MS. 1996. Acetylcholinesterase staining in human auditory and language cortices: regional variation of structural features. Cereb Cortex. 6:260–270.

Jensen O, Mazaheri A. 2010. Shaping functional architecture by oscillatory alpha activity: gating by inhibition. Front Hum Neurosci. 4:186.

Keil J, Müller N, Ihssen N, Weisz N. 2012. On the variability of the McGurk effect: audiovisual integration depends on prestimulus brain states. Cereb Cortex. 22:221–231.

Klimesch W, Sauseng P, Hanslmayr S. 2007. EEG alpha oscillations: the inhibition-timing hypothesis. Brain Res Rev. 53:63–88.

Knudsen EI, Brainard MS. 1995. Creating a unified representation of visual and auditory space in the brain. Annu Rev Neurosci. 18:19–43.

Lamme VAF. 2006. Towards a true neural stance on consciousness. Trends Cogn Sci. 10:494–501.

Lange J, Keil J, Schnitzler A, van Dijk H, Weisz N. 2014. The role of alpha oscillations for illusory perception. Behav Brain Res. 271:294–301.

Lange J, Oostenveld R, Fries P. 2013. Reduced occipital alpha power indexes enhanced excitability rather than improved visual perception. J Neurosci. 33:3212–3220.

Maris E, Oostenveld R. 2007. Nonparametric statistical testing of EEG- and MEG-data. J Neurosci Methods. 164:177–190.

Melloni L, Molina C, Pena M, Torres D, Singer W, Rodriguez E. 2007. Synchronization of neural activity across cortical areas correlates with conscious perception. J Neurosci. 27: 2858–2865.

Müller N, Weisz N. 2012. Lateralized auditory cortical alpha band activity and interregional connectivity pattern reflect anticipation of target sounds. Cereb Cortex. 22:1604–1613.

Nolte G. 2003. The magnetic lead field theorem in the quasi-static approximation and its use for magnetoencephalography forward calculation in realistic volume conductors. Phys Med Biol. 48:3637–3652.

Nolte G, Bai O, Wheaton L, Mari Z, Vorbach S, Hallett M. 2004. Identifying true brain interaction from EEG data using the imaginary part of coherency. Clin Neurophysiol. 115: 2292–2307.

Oostenveld R, Fries P, Maris E, Schoffelen J-M. 2011. FieldTrip: open source software for advanced analysis of MEG, EEG, and invasive electrophysiological data. Comput Intell Neurosci. 2011:156869.

Palva S, Palva JM. 2012. Discovering oscillatory interaction networks with M/EEG: challenges and breakthroughs. Trends Cogn Sci. 16:219–230.

Penhune VB, Zatorre RJ, MacDonald JD, Evans AC. 1996. Interhemispheric anatomical differences in human primary auditory cortex: probabilistic mapping and volume measurement from magnetic resonance scans. Cereb Cortex. 6:661–672.

Popov T, Miller GA, Rockstroh B, Weisz N. 2013. Modulation of α power and functional connectivity during facial affect recognition. J Neurosci. 33:6018–6026.

Recanzone GH. 2003. Auditory influences on visual temporal rate perception. J Neurophysiol. 89:1078–1093.

Romei V, Brodbeck V, Michel C, Amedi A, Pascual-Leone A, Thut G. 2008. Spontaneous fluctuations in posterior alpha-band EEG activity reflect variability in excitability of human visual areas. Cereb Cortex. 18:2010–2018.

Romei V, Gross J, Thut G. 2012. Sounds reset rhythms of visual cortex and corresponding human visual perception. Curr Biol. 22:807–813.

Rubinov M, Sporns O. 2010. Complex network measures of brain connectivity: uses and interpretations. Neuroimage. 52:1059–1069.

Ruhnau P, Hauswald A, Weisz N. 2014. Investigating ongoing brain oscillations and their influence on conscious perception – network states and the window to consciousness. Front Psychol. 5:1–9.

Sadaghiani S, Hesselmann G, Kleinschmidt A. 2009. Distributed and antagonistic contributions of ongoing activity fluctuations to auditory stimulus detection. J Neurosci. 29:13410–13417.

Sauseng P, Klimesch W, Gerloff C, Hummel FC. 2009. Spontaneous locally restricted EEG alpha activity determines cortical excitability in the motor cortex. Neuropsychologia. 47:284–288.

Seldon HL. 1981a. Structure of human auditory cortex. I. Cytoarchitectonics and dendritic distributions. Brain Res. 229: 277–294.

Seldon HL. 1981b. Structure of human auditory cortex. II. Axon distributions and morphological correlates of speech perception. Brain Res. 229:295–310.

Seldon HL. 1982. Structure of human auditory cortex. III. Statistical analysis of dendritic trees. Brain Res. 249:211–221.

Singer W. 2011. Dynamic formation of functional networks by synchronization. Neuron. 69:191–193.

Spaak E, de Lange FP, Jensen O. 2014. Local entrainment of α oscillations by visual stimuli causes cyclic modulation of perception. J Neurosci. 34:3536–3544.

Steinmann S, Leicht G, Mulert C. 2014. Interhemispheric auditory connectivity: structure and function related to auditory verbal hallucinations. Front Hum Neurosci. 8:55.

Van Dijk H, Schoffelen J-M, Oostenveld R, Jensen O. 2008. Prestimulus oscillatory activity in the alpha band predicts visual discrimination ability. J Neurosci. 28:1816–1823.

Van Veen BD, van Drongelen W, Yuchtman M, Suzuki A. 1997. Localization of brain electrical activity via linearly constrained minimum variance spatial filtering. IEEE Trans Biomed Eng. 44:867–880.

Van Wijk BCM, Stam CJ, Daffertshofer A. 2010. Comparing brain networks of different size and connectivity density using graph theory. PLoS One. 5:e13701.

Von Békésy G. 1960. Experiments in hearing. New York: McGraw-Hill Book Co.

Weisz N, Wühle A, Monittola G, Demarchi G, Frey J, Popov T, Braun C. 2014. Prestimulus oscillatory power and connectivity patterns predispose conscious somatosensory perception. Proc Natl Acad Sci USA. 111:E417–E425.

Zatorre RJ. 2001. Spectral and temporal processing in human auditory cortex. Cereb Cortex. 11:946–953.

Zatorre RJ, Belin P, Penhune VB. 2002. Structure and function of auditory cortex: music and speech. Trends Cogn Sci. 6:37–46.

Zatorre RJ, Penhune VB. 2001. Spatial localization after excision of human auditory cortex. J Neurosci. 21:6321–6328.

Zeki S, Bartels A. 1999. Toward a theory of visual consciousness. Conscious Cogn. 8:225–259.